ELSEVIER

Polymer 40 (1999) 887–893

polymer

Electroactive polymer–SiO_2 nanocomposites for metal uptake

K.G. Neoh[a,]*, K.K. Tan[a], P.L. Goh[a], S.W. Huang[a], E.T. Kang[a], K.L. Tan[b]

[a]Department of Chemical Engineering, National University of Singapore, Kent Ridge 119260, Singapore
[b]Department of Physics, National University of Singapore, Kent Ridge 119260, Singapore

Received 12 February 1998; revised 15 April 1998; accepted 15 April 1998

Abstract

The use of electroactive polymer–SiO_2 nanocomposites for the uptake of gold and palladium from $AuCl_3$ and $PdCl_2$ in acid solutions respectively was investigated. The electroactive polymers used were polyaniline (PAN) and polypyrrole (PPY). The change in the physicochemical properties of the nanocomposites with metal uptake were of particular interest. In the case of gold uptake, the reaction rate increases with temperature from 0 to 60°C. The accumulation of elemental gold on the nanocomposites increases the diameter and decreases the surface area. The surface Au/N ratio as determined using X-ray photoelectron spectroscopy (XPS) is highly dependent on the rate of reactions even for the same amount of gold uptake. The uptake of palladium from $PdCl_2$ is much more difficult to accomplish. High rates of uptake can only be achieved with the electroactive polymers reduced to their lowest oxidation state and unlike the case of gold uptake, the palladium on the microparticles does not exist in the elemental form but as a Pd(II) compound. © 1998 Elsevier Science Ltd. All rights reserved.

Keywords: Electroactive polymer; Nanocomposites; Metal uptake

1. Introduction

A number of processes have been investigated for the recovery of precious metals from primary and secondary sources with the aim of minimizing energy requirements and adverse environmental impact [1]. Examples of such processes include reduction or accumulation by polymeric adsorbents [2,3], by biomass and biomaterials [4–6], by activated carbon [7] and by electroless plating [8]. Spontaneous deposition of palladium and silver on polyaniline (PAN) substrate has also been reported [9]. We have recently shown that by coupling the changes in the intrinsic oxidation state of electroactive polymers such as PAN and polypyrrole (PPY) and their protonation and reduction in acid solution with the decrease in the oxidation state of the metal, electroless precipitation of gold in elemental form from acid solutions can be achieved [10,11]. A comparison of the reduction of gold from chloroauric acid solution by PPY films and powders clearly demonstrated the effect of surface area limitation on this process [10].

Recently, PAN and PPY have been synthesized in the form of nanocomposites using ultra-fine SiO_2 particles [12,13]. These materials have potential commercial applications [14] and in this paper we describe the use of these materials for metal uptake. Our interest in these materials stems from the fact that they possess a surface area substantially higher than that estimated from the particle size [14] and hence could aid the process of metal uptake. In addition, the distribution of catalytic particles such as platinum or palladium on high surface area substrates can result in potential advantages when used in catalytic applications [15]. The emphasis of this paper is on the changes in the physicochemical properties of these microparticles as they interact with metal ions in solutions. Various analytical techniques such as X-ray photoelectron spectroscopy (XPS), thermogravimetric analysis, particle size and surface area measurements were employed to characterize the microparticles in this work.

2. Experimental

2.1. Synthesis of nanocomposites

The procedures for the synthesis of the PAN–SiO_2 and PPY–SiO_2 nanocomposites essentially followed those reported by Armes and co-workers [12,13]. In the synthesis of the PAN–SiO_2 nanocomposites, 7.2 ml colloidal silica in the form of 34% by weight SiO_2 aqueous suspension (Ludox TMA from Aldrich Chemical Co.) was first added to 100 ml of 1 M HCl containing 3.14 g $(NH_4)_2S_2O_8$. Aniline (2 ml) was then injected into the solution under constant stirring and the polymerization was allowed to proceed for 2 h. The

---

* Corresponding author.

PII S0032-3861(98)00297-3

reaction mixture was then centrifuged at 6000 rev min^{-1} for 30 min. The supernatant was discarded and the resulting dark green sediment was redispersed in 1 M HCl using an ultrasonic bath. The centrifugation–redispersion cycle was repeated twice more to completely remove the excess small silica particles from the larger PAN–SiO_2 nanocomposites. The microparticles were then stored as a suspension in 1 M HCl. In the case of PPY–SiO_2 nanocomposites, the procedure was similar with 7.2 ml of colloidal silica being added to 100 ml of deionized water and 9.1 g $FeCl_3 \cdot 6H_2O$ followed by 1 ml of pyrrole. The polymerization was allowed to proceed for 16 h and the process for washing and storing the PPY–SiO_2 nanocomposites was the same as that described above for PAN–SiO_2 except that deionized water was used.

2.2. Uptake of metal from solutions

Solutions with different gold concentrations were prepared by diluting chloroauric acid solution containing 1000 mg dm^{-3} of Au in 0.5 M HCl (supplied by BDH Chemicals). Palladium chloride solution (5 wt% $PdCl_2$ in 10% HCl) was purchased from Aldrich Chemicals and diluted to various palladium concentrations in 0.5 M HCl. The metal uptake experiments were conducted using a range of N (from PPY or PAN)/metal mole ratios. The volume of microparticles suspension added to the chloride solution was calculated from the N/metal concentration, the solid content of the suspension and the polymer content of the microparticles (see later section). Typically, for an N/metal mole ratio of 2:1 about 1 ml of suspension was added to 100 ml of solution with 100 mg dm^{-3} metal ion. After the microparticles were added to the solution (under constant stirring), samples of the solution were removed at regular intervals for the determination of the gold or palladium chloride concentration using ultraviolet (UV)–visible absorption spectroscopy (Shimadzu UV-160A spectrophotometer). The microparticles were removed by centrifugation prior to the absorption measurements. The absorbance was monitored at 314 nm for gold chloride and 280 nm for palladium chloride, and compared to the standard calibration curve. After various reaction times, the microparticles were also removed by centrifugation and dried under reduced pressure.

2.3. Characterization of microparticles

The microparticles were stored as a suspension in 0.5 M HCl (for PAN–SiO_2) or deionized water (for PPY– SiO_2) prior to the metal uptake experiments. The solid content of the suspension was determined from the density of the suspension and the weight remaining after a known volume was heated to dryness at 60°C. To determine the polymer content of the microparticles, a known weight (≈ 40 mg) of microparticles was heated to 800°C at 20°C min^{-1} in 120 ml min^{-1} of air in a Netzsch STA 409 simultaneous thermogravimetric differential thermal analyser. To ensure complete combustion of the organic material, the temperature was maintained at 800°C for 20 min. BET surface area measurements were carried out using a Quantachrome NOVA1000 with N_2 as the adsorbate. The particle size distributions were determined from photon correlation spectroscopy using the Zeta Plus analyser from Brookhaven Instruments.

XPS measurement on all samples were made on a VG ESCALAB MkII spectrometer with an Mg Kα X-ray source (1253.6 eV photons). The X-ray power supply was run at a reduced power of 120 W (12 kV and 10 mA). The samples were mounted on the standard sample studs using double-sided tapes. The pressure in the analysis chamber during each measurement was maintained at 10^{-8} mbar or less. Core-level scans of carbon (C1s), nitrogen (N1s), oxygen (O1s), sulfur (S2p), chlorine (Cl2p), gold (Au4f) and palladium (Pd3d) were made on the samples. To compensate for the surface charging in less conductive samples, all XPS spectra were referenced to the C1s neutral carbon at 284.6 eV. In peak synthesis, the full-widths at half-maximum of Gaussian peaks were kept constant for all components in a particular spectrum. Relative surface elemental stoichiometries were obtained from the peak area ratios of the various elements corrected with the appropriate instrument sensitivity factors and are accurate to ± 10%.

3. Results and discussion

3.1. Properties of microparticles

The polymer content of the microparticles as determined by thermogravimetric analysis and the chemical composition as calculated from the XPS core-level area ratios of the various elements (after correction with sensitivity factors) are given in Table 1. The N/C ratios are slightly lower than those expected for PAN (0.167) and PPY (0.25). The chlorine present in the microparticles exists predominantly as Cl^- anions as indicated by the peak in the 197 eV binding

Table 1
Chemical composition, effective particle size and specific surface area of PAN–SiO_2 and PPY–SiO_2 nanocomposites

Type of micro particles	Polymer content (wt%)	Surface composition			Particle size (nm)	Specific surface area (m^2 g^{-1})
		N/C	Cl/N	Si/N		
PAN–SiO_2	44.0	0.14	0.33	14.5	530	72
PPY–SiO_2	37.8	0.20	0.26	15.0	320	91

energy region. The surface Si/N ratios as determined by XPS are very much higher compared to the overall composition value (Si/N $\approx$ 2) estimated from thermogravimetric analysis, confirming an SiO_2-rich surface. Maeda et al. [16] have also shown that the surface Si/N ratio can be more than eight times higher than the bulk value. The effective particle size determined in this work (based on the light scattering technique) is about twice those reported by Maeda and Armes for PAN–SiO_2 and PPY–SiO_2 nanocomposites having similar polymer content [14]. The differences in the type of colloidal silica and the techniques employed for particle size determination may result in differences in values, especially since the light scattering technique is sensitive to the presence of aggregates. The colloidal silica used in this work was determined to have an effective diameter of 180 nm which is significantly larger than those used by Armes et al. (reported to be 38 nm). The specific surface areas of the PAN–SiO_2 and PPY–SiO_2 nanocomposites as determined by the BET technique are about an order of magnitude higher than those based on the particle size and assuming a spherical morphology and a particle density of 2 g cm^{-3}, indicating a high degree of porosity in the microparticles[14].

3.2. Uptake of gold

The rates of gold uptake from chloroauric acid (as indicated by the decrease of the gold concentration in solution) by PAN–SiO_2 nanocomposites and PAN powder are compared in Fig. 1. The weights of PAN in both samples were kept the same. The PAN powder was synthesized in the same manner as the PAN–SiO_2 nanocomposites except that colloidal silica was not used. Experiments conducted with the colloidal silica (i.e. in the absence of the electroactive polymers) show that the silica plays no direct role in the uptake of gold from the chloroauric solution. The similarity in the rates indicates that the low surface N/Si ratio of the PAN–SiO_2 nanocomposites is compensated by the higher surface area available as compared to the case of the PAN powder. The specific surface area of PAN–SiO_2 is about twice that of PAN powder. In the case of PPY–SiO_2 nanocomposites, the rate is slightly lower than that of PPY powder (keeping the same polymer content).

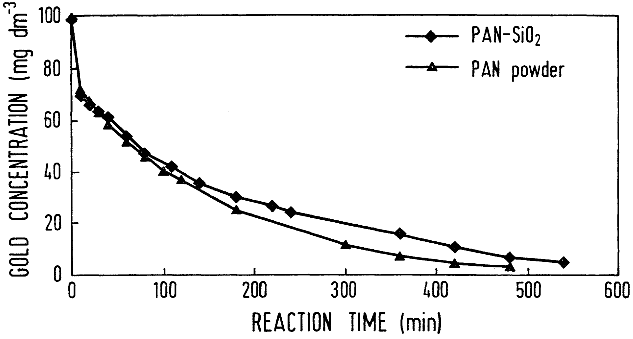

Fig. 1. Comparison of rates of gold uptake from chloroauric acid solution by PAN powder and PAN–SiO_2 nanocomposites: $(N/Au)_{initial} = 0.7:1$, $T = 25°C$.

The rates of gold uptake by the PAN–SiO_2 and PPY–SiO_2 nanocomposites are compared in Fig. 2. In both cases, the concentration of gold ions in solution decreased by about 50% within the first 15 min. The PAN–SiO_2 nanocomposites are more effective in the uptake of gold, achieving a 94% reduction within 200 min (Fig. 2(a)) compared to 80% reduction by the PPY–SiO_2 nanocomposites (Fig. 2(b)) in the same time span. The decrease in the rate of gold uptake with time is attributed to the decreasing gold concentration in solution and the loss of effective surface area for reaction. The latter effect is clearly demonstrated when the gold concentration is brought back to 100 mg dm^{-3} with the addition of a small amount (less than 10% of the reaction mixture's volume) of 1000 mg dm^{-3} chloroauric acid (Fig. 2).

The XPS C1s, N1s and Au4f core-level spectra of the pristine PAN–SiO_2 nanocomposites and those after 24 h in chloroauric acid (100 mg dm^{-3} Au) are shown in Fig. 3. The C1s core-level spectra (Fig. 3(a) and Fig. 3(b)) indicate a slight increase in the oxidized C species, mainly C–O and O=C–O after the gold uptake experiment. The PAN remains fully protonated (i.e. no –N= peak is observed in the N1s spectra). The presence of the $Au4f_{7/2}$ peak in the 84 eV region (Fig. 3(f)) confirms that the gold is present in the elemental form [17] on the microparticles. Fig. 4 shows the corresponding core-level spectra for the PPY–SiO_2 nanocomposites before and after the gold uptake experiments. A small amount of unprotonated –N= (BE of 397.7 eV) was present in the pristine PPY–SiO_2 nanocomposites which is attributed to the loss of anions when the

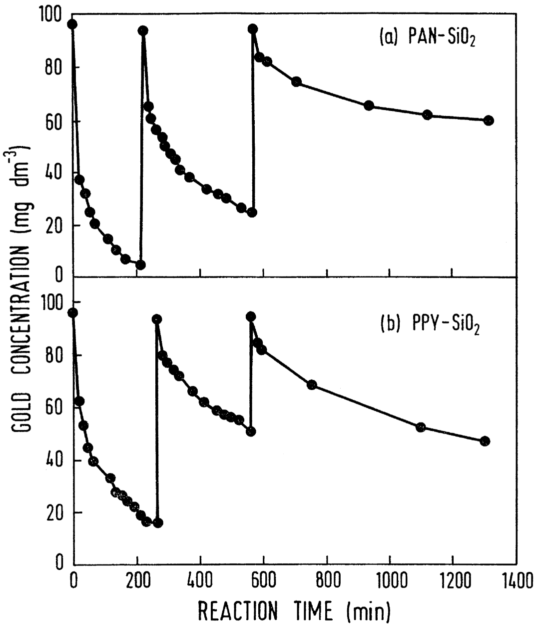

Fig. 2. Three cycles of gold uptake from chloroauric acid solution by (a) PAN–SiO_2 nanocomposites and (b) PPY–SiO_2 nanocomposites: $(N/Au)_{initial} = 2:1$, $T = 25°C$.

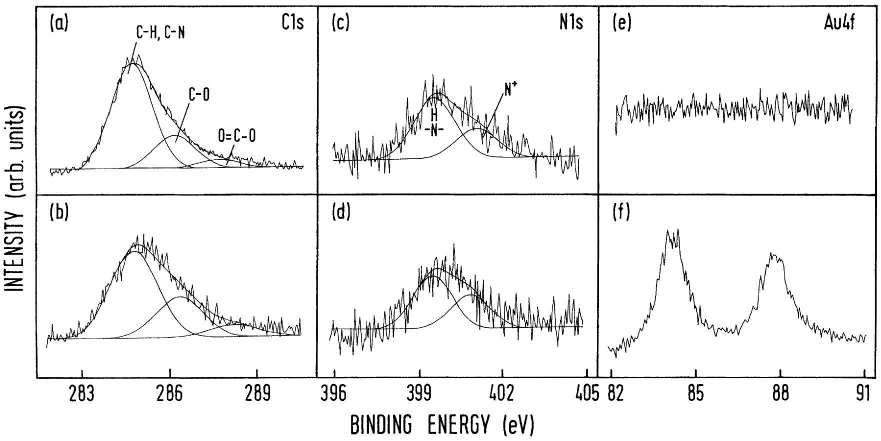

Fig. 3. XPS core-level spectra of pristine PAN–SiO_2 nanocomposites ((a), (c), (e)) and PAN–SiO_2 nanocomposites after 24 h in chloroauric acid solution ((b), (d), (f)). Gold uptake carried out using $(N/Au)_{initial} = 2:1$ at $T = 25°C$.

microparticles are washed with deionized water after synthesis. This undoping process was not observed with the PPY–SiO_2 nanocomposites after the gold uptake experiment because the experiment was conducted in 0.5 M HCl and no washing with water was carried out after centrifugation. As in the case of the PAN–SiO_2 nanocomposites, the gold deposited on the PPY–SiO_2 nanocomposites is in the elemental form.

The surface Au/N ratios of the PAN–SiO_2 nanocomposites and PPY–SiO_2 nanocomposites as calculated from the peak area ratios in the XPS analyses are compared with the Au/N ratios calculated from the amount of Au uptake from the chloroauric solution for two sets of conditions in Table 2. In both Runs A and B, the initial mole ratio of N (in the microparticles) to gold ions in solution is 2:1 and the reactions are carried out until at least 90% of the gold in the solution is taken up by the microparticles (as shown by the decrease in the absorbance band at 314 nm). In Run A, the surface Au/N ratios of the microparticles are significantly lower than the values calculated from the amount of gold uptake from solution. The latter were also compared with the bulk Au/N ratios calculated from thermogravimetric analysis assuming the polymer/SiO_2 ratios of the microparticles were not changed by the reactions occurring during gold uptake. The bulk Au/N ratios determined from thermogravimetric analysis are 0.50 and 0.49 for PAN–SiO_2 nanocomposites and PPY–SiO_2 nanocomposites, respectively, which are in good agreement with the values calculated from the gold uptake from solution. The particle size after gold uptake increases substantially and the specific surface area correspondingly decreases (comparing Table 2 with Table 1).

The results discussed above for Run A were obtained with a relatively diluted chloroauric solution and the microparticles were separated from the solution after the experiment by centrifugation. It is possible that the elemental gold deposited on the microparticles may be separated from the microparticles during the centrifugation process, especially if a thick coating of gold has been formed. Thus, Run B was conducted with the concentration of gold ions in solution being 10 times higher than Run A but keeping the same total amount of gold ions and N/Au ratio. At the end of the experiment, the mixture was slowly heated to dryness. The surface Au/N ratios of the microparticles for Run B

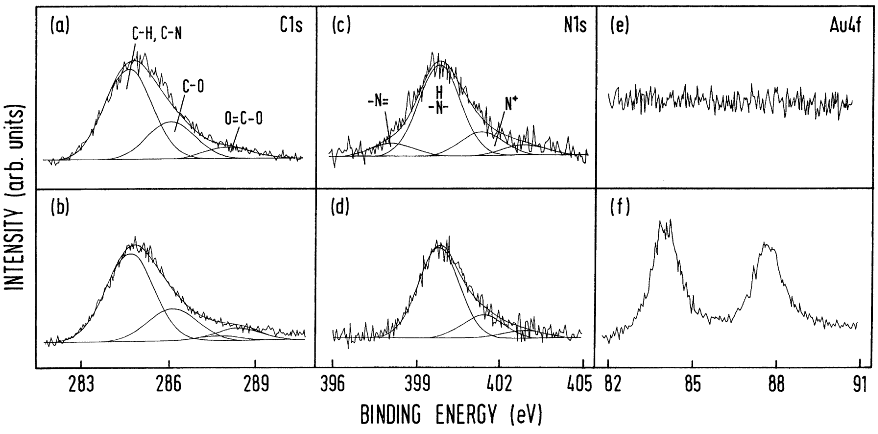

Fig. 4. XPS core-level spectra of pristine PPY–SiO_2 nanocomposites ((a), (c), (e)) and PPY–SiO_2 nanocomposites after 24 h in chloroauric acid solution ((b), (d), (f)). Gold uptake carried out using $(N/Au)_{initial} = 2:1$ at $T = 25°C$.

Table 2
Effect of gold uptake on composition and properties of PAN–SiO_2 and PPY–SiO_2 nanocomposites

Type of microparticles	Chloroauric solution	Centrifugation	Surface composition				$(Au/N)^a_{calc.}$	Particle size (nm)	Specific surface area ($m^2\ g^{-1}$)
			N/C	Cl/N	Si/N	Au/N			
PAN–SiO_2									
Run A	100 ml of 100 mg dm^{-3} Au	Yes	0.13	0.33	17.3	0.15	0.47	1800	44
Run B	10 ml of 1000 mg dm^{-3} Au	No	0.17	0.32	19.4	0.92	0.48	2300	44
PPY–SiO_2									
Run A	100 ml of 100 mg dm^{-3} Au	Yes	0.19	0.44	11.8	0.27	0.45	2400	44
Run B	10 ml of 1000 mg dm^{-3} Au	No	0.19	0.35	13.6	0.76	0.49	4700	54

[a] Calculated from the decrease in gold concentration in the chloroauric solution.

were found to be significantly higher than the bulk Au/N ratios, in contrast to the results from Run A (Table 2). The particle sizes are also substantially higher than those from Run A but the surface areas are either similar or higher. It should be mentioned that particle sizes beyond 3000 nm cannot be determined accurately using the technique employed, hence the value reported for PPY–SiO_2 in Run B is at best an estimate. The higher surface Au/N ratios and particle sizes obtained in Run B compared to Run A may indicate that gold deposited on the microparticles is dislodged during centrifugation in Run A. Alternatively, the higher gold ion concentration in solution in Run B results in an increase in reaction rate with a concomitant rapid deposition of gold on the surface of the microparticles and less reaction occurring in the bulk, and also possibly a higher degree of aggregation.

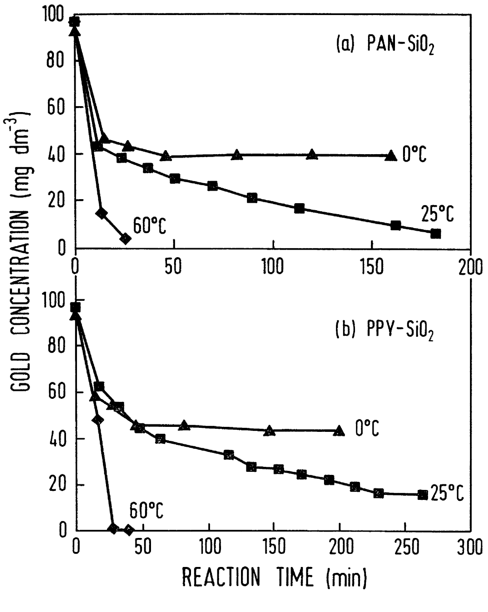

Fig. 5. Effect of temperature on gold uptake from chloroauric acid solution by (a) PAN–SiO_2 nanocomposites and (b) PPY–SiO_2 nanocomposites. $(N/Au)_{initial} = 2:1$).

The results presented above were obtained at room temperature (25°C). It was noticed during the course of the gold uptake experiments that the reaction mixture cooled down, implying the reactions are endothermic. Experiments were then conducted at different temperatures and the rates of gold uptake were found to be highly dependent on temperature, as illustrated in Fig. 5(a), Fig. 5(b) for the PAN–SiO_2 and PPY–SiO_2 nanocomposites, respectively. At 0°C, for both types of particles, the reaction slows down greatly after 45 min and the gold concentration in solution reaches an asymptotic value close to 40 mg dm^{-3}, whereas at 60°C essentially all the gold ions have been reduced to elemental gold in the same time span. The higher reaction rate at 60°C also resulted in significantly higher surface Au/N ratios than those obtained at 25°C even though the total gold uptake from solution in both cases is almost the same. The surface Au/N ratios (from XPS) for the PAN–SiO_2 and PPY–SiO_2 nanocomposites after gold uptake at 60°C are 2.3 and 0.97 respectively compared to the corresponding values of 0.15 and 0.27 obtained at 25°C.

We have earlier proposed that the reduction of gold from acid solution and the subsequent accumulation of elemental gold on PAN [10] and PPY [11] involve the initial oxidation of the polymer to a higher intrinsic oxidation state. In the acid solution, the subsequent reprotonation of the highly oxidized state will result in a reduction of the PAN to the 50% oxidized state and PPY to the 25% oxidized state. Experiments were also conducted to test whether the reaction rates were affected by the presence of O_2. The results showed that the rates of gold uptake are similar when the experiments were conducted in air or under an N_2 atmosphere, thus indicating that O_2 plays no significant role in the oxidation–reprotonation–reduction cycle of the electroactive polymers in chloroauric solution.

3.3. Uptake of palladium

The uptake of palladium from the palladium chloride solution by PAN–SiO_2 and PPY–SiO_2 nanocomposites is

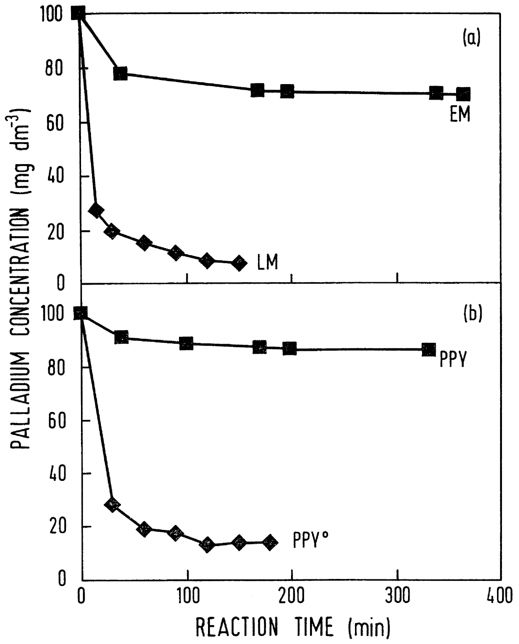

Fig. 6. Effect of oxidation state of (a) PAN and (b) PPY in the microparticles on the uptake of palladium from palladium chloride solution $(N/Pd)_{initial} = 2:1$).

much slower than the uptake of gold (compare EM curve in Fig. 6(a) and PPY curve in Fig. 6(b) with the first cycle curves in Fig. 2(a), Fig. 2(b)). Unlike the case of gold uptake, increasing the reaction temperature to 60°C did not result in any significant increase in the uptake of palladium. An attempt was made to increase the rates of palladium uptake by decreasing the oxidation state of the electroactive polymers in the microparticles. In the as-synthesized PAN–SiO_2 nanocomposites, the PAN is expected to be close to the emeraldine (EM or 50% oxidized) state. Although the N1s core-level spectrum in Fig. 3(c) indicates an –NH–/N ratio significantly greater than 0.5, our earlier work has shown that in the high vacuum environment during the XPS measurements, the loss of volatile dopant (in this case, HCl) may result in an increase in –NH– groups [18]. In the as-synthesized PPY–SiO_2 nanocomposites, the PPY is likely to be in the 75% reduced form. The conversion of the electroactive polymers in the as-synthesized PAN–SiO_2 and PPY–SiO_2 nanocomposites to the fully reduced form (i.e. all –NH– units) was carried out in a two-step process: undoping of the polymers to the base form using excess NaOH solution followed by treatment with hydrazine. The N1s core-level spectra of the PAN–SiO_2 and PPY–SiO_2 after reduction by hydrazine (denoted as LM–SiO_2 and PPY°–SiO_2, respectively) are shown in Fig. 7(a), Fig. 7(b). The predominant peak component attributable to the –NH– groups and the barely discernible N^+ peak component in Fig. 7(a) are characteristic of leucoemeraldine (LM)[19]. Comparing Fig. 7(b) with Fig. 4(c), it can be seen that the –N = component is absent in the former, but the intensity of the N^+ peak component in Fig. 7(b) remains substantial due to the ease in which reduced neutral PPY (PPY°) is doped by reaction with oxygen [20]. The palladium uptake rates achieved using the fully reduced form of PAN (leucoemeraldine) and PPY (denoted by the LM and PPY° curves in Fig. 6(a), Fig. 6(b) respectively) in the microparticles are very much higher than those observed with the as-synthesized PAN–SiO_2 and PPY–SiO_2 nanocomposites. As in the case of gold uptake, polyaniline is slightly more effective than polypyrrole in the uptake of palladium.

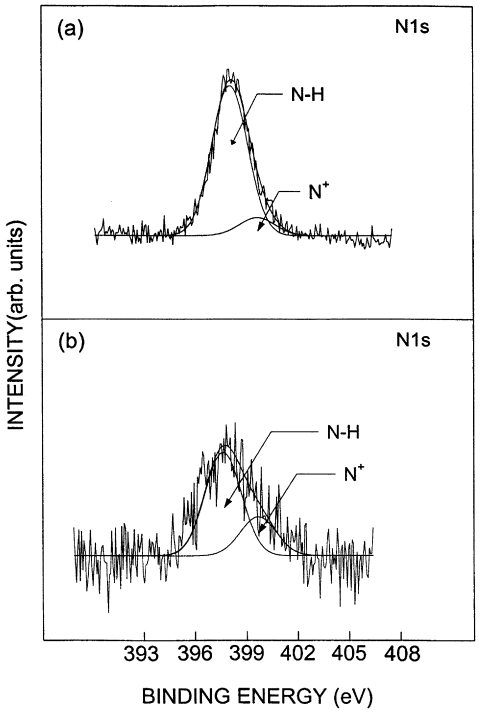

Fig. 7. XPS N1s core-level spectra of (a) LM–SiO_2 and (b) PPY°–SiO_2.

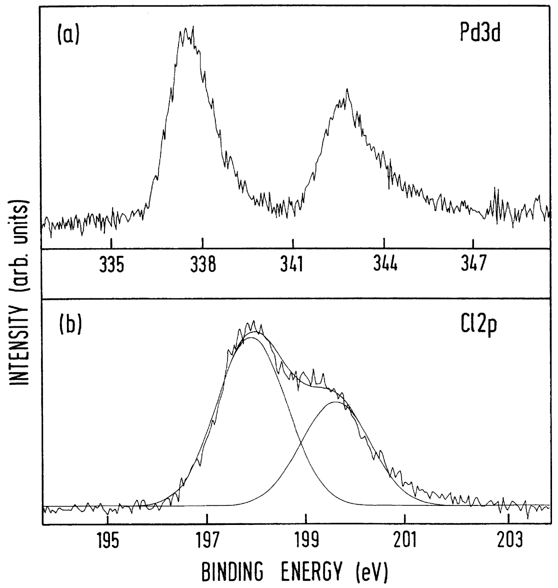

Fig. 8. XPS core-level spectra of LM–SiO_2 nanocomposites after Pd uptake.

The Pd3d core–level spectra of the LM–SiO_2 and PPY°–SiO_2 nanocomposites after reaction in the acidic $PdCl_2$ solution show a $Pd3d_{5/2}$ peak component around 337.5 eV (Fig. 8(a)) characteristic of Pd(II) [21]. Thus, unlike the case of $AuCl_3$, the Pd(II) is not reduced to the elemental state (BE of the $Pd3d_{5/2}$ component of Pd(0) is at 335 eV). The Cl2p core-level spectra of the corresponding samples show a $Cl2p_{3/2}$ peak component at 198 eV (Fig. 8(b)). The position of this $Cl2p_{3/2}$ peak component agrees with the corresponding Cl2p peak component obtained when $PdCl_2$ is used for calibration. The Cl/Pd ratio in the LM–SiO_2 and PPY°–SiO_2 nanocomposites after reaction in the acidic $PdCl_2$ solution is also close to two. The Pd content in the microparticles is not significantly affected when the microparticles are soaked in water for 24 h followed by washing with copious amounts of water. The mechanism of $PdCl_2$ uptake is not clear at the present moment. It is possible that $PdCl_2$ from the acid solution forms a complex with the LM and PPY° electroactive polymers in the microparticles. The ability of palladium chloride and platinum chloride (in the form of Pd_6Cl_{12} and Pt_6Cl_{12}) to form complexes with electron donors has been reported previously [22]. From our results (Fig. 6), it appears that the oxidation state of the polymer plays a very significant role in the reaction with $PdCl_2$ in solution. The ability to immobilize $PdCl_2$ on the microparticles can lead to potential applications since Pd(II) compounds as well as Pd(0) are used as catalysts in organic synthesis. Work is currently being carried out to determine the catalytic activity of these Pd-containing microparticles.

4. Conclusion

The PAN–SiO_2 and PPY–SiO_2 nanocomposites used in this study are rich in Si on the surface compared to the bulk but they possess a high surface area for reaction. In the uptake of gold from chloroauric acid by PAN–SiO_2 and PPY–SiO_2, a slightly higher rate is achieved with the PAN–SiO_2. The reaction rates are highly dependent on temperature in the range of 0 to 60°C but are not sensitive to O_2. The reactions resulted in the accumulation of elemental gold on the microparticles which causes an increase in particle diameter and reduction in surface area. The surface Au/N ratio can be higher or lower than the bulk value depending on the reaction conditions. A high reaction rate results in a surface Au/N ratio which is substantially higher than the bulk value. The uptake of palladium from acid solution is more difficult to accomplish than for gold uptake. The rate of uptake is low for as-synthesized PAN–SiO_2 and PPY–SiO_2 nanocomposites, but increases rapidly when the PAN and PPY are reduced to their lowest oxidation state. However, XPS analysis clearly shows that the palladium in the microparticles exists in the Pd(II) state and the Cl/Pd ratio is close to two. It is possible that palladium chloride has undergone complexation with the electroactive polymers in their lowest oxidation state. The results showed that the electroactive polymer–SiO_2 nanocomposites represent a potentially useful material not only for recovery of precious metal but also for catalytic applications.

References

[1] Arbiter N, Han KN. Gold—advances in precious metals recovery. New York: Gordon and Breach, 1990.
[2] Asker M, Wan RY, Miller JD. Solv Extract Ion Exch 1986;4:531.
[3] Fritz JS, Miller WG. US Patent No. 3736126. 1973.
[4] Kuyucak N, Volesky B. Biorecovery 1989;1:189.
[5] Watkins JW, Elder RC, Greene B, Darnall DW. Inorg Chem 1987;26:1147.
[6] Hosea M, Greene B, McPherson R, Henzl M, Alexander MD, Darnall DW. Inorg Chem Acta 1986;123:161.
[7] McDougall GJ, Hancock RD. Miner Sci Eng 1980;12:85.
[8] Okinawa Y. In: Reid F, Goldie W, editors. Gold plating technology. New York: Electrochemical, 1974, Chapter 11.
[9] Huang WS, Angelopoulos M, White JR, Park JM. Mol Cryst Liq Cryst 1990;189:227.
[10] Ting YP, Neoh KG, Kang ET, Tan KL. J Chem Tech Biotech 1994;59:31.
[11] Kang ET, Ting YP, Neoh KG, Tan KL. Synth Met 1995;69:477.
[12] Maeda S, Armes SP. J Colloid Interface Sci 1993;159:257.
[13] Gill M, Mykytiuk J, Armes SP, Edwards JL, Yeates T, Moreland PJ, Mollet C. J Chem Soc, Chem Commun 1992:108.
[14] Maeda S, Armes SP. Synth Met 1995;73:151.
[15] Bauer L, Fisch H, Haas K. European Patent No. 665265 A2. 1995.
[16] Maeda S, Gill M, Armes SP, Fletcher IW. Langmuir 1995;11:1899.
[17] Chastain J, editor. Handbook of X-ray photoelectron spectroscopy. Eden Prairie, MN: Perkin-Elmer, 1992:183.
[18] Neoh KG, Kang ET, Tan KL. J Phys Chem 1991;95:10151.
[19] Tan KL, Tan BTG, Kang ET, Neoh KG. Phys Rev 1989;39:8070.
[20] Street GB, Clarke TC, Krounbi M, Kanazawa K, Lee V, Pfluger P, Scott JC, Weiser G. Mol Cryst Liq Cryst 1982;83:253.
[21] Chastain J, editor. Handbook of X-ray photoelectron spectroscopy. Eden Prairie, MN: Perkin-Elmer, 1992:119.
[22] Maitlis PM. Metal complexes. In: The organic chemistry of palladium, vol. 1. New York: Academic Press, 1971:45.